Accepted Manuscript

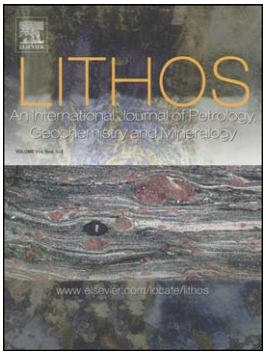

Assembly of the Lhasa and Qiangtang terranes in central Tibet by divergent double subduction

Di-Cheng Zhu, Shi-Min Li, Peter A. Cawood, Qing Wang, Zhi-Dan Zhao, Sheng-Ao Liu, Li-Quan Wang

PII: S0024-4937(15)00232-7
DOI: doi: 10.1016/j.lithos.2015.06.023
Reference: LITHOS 3632

To appear in: *LITHOS*

Received date: 4 May 2015
Accepted date: 29 June 2015

Please cite this article as: Zhu, Di-Cheng, Li, Shi-Min, Cawood, Peter A., Wang, Qing, Zhao, Zhi-Dan, Liu, Sheng-Ao, Wang, Li-Quan, Assembly of the Lhasa and Qiangtang terranes in central Tibet by divergent double subduction, *LITHOS* (2015), doi: 10.1016/j.lithos.2015.06.023

Assembly of the Lhasa and Qiangtang terranes in central Tibet by divergent double subduction

Di-Cheng Zhu[1,*], Shi-Min Li[1], Peter A. Cawood[2,3], Qing Wang[1], Zhi-Dan Zhao[1], Sheng-Ao Liu[1], Li-Quan Wang[4]

1. State Key Laboratory of Geological Processes and Mineral Resources, and School of Earth Science and Resources, China University of Geosciences, Beijing 100083, China
2. Department of Earth Sciences, University of St Andrews, North Street, St Andrews KY16 9AL, UK
3. Centre for Exploration Targeting, School of Earth and Environment, University of Western Australia, 35 Stirling Hwy, Crawley WA, 6009, Australia
4. Chengdu Institute of Geology and Mineral Resources, Chengdu 610082, China

Revised manuscript submitted to Lithos (June 12, 2015)

*Corresponding author: **Di-Cheng Zhu**

State Key Laboratory of Geological Processes and Mineral Resources

China University of Geosciences

29# Xue-Yuan Road, Haidian District

Beijing 100083, China

Phone: (+86-10) 8232 2094 (O)

Fax: (+86-10) 8232 2094

Email: dchengzhu@163.com

Abstract

Integration of lithostratigraphic, magmatic, and metamorphic data from the Lhasa-Qiangtang collision zone in central Tibet (including the Bangong suture zone and adjacent regions of the Lhasa and Qiangtang terranes) indicates assembly through divergent double sided subduction. This collision zone is characterized by the absence of Early Cretaceous high-grade metamorphic rocks and the presence of extensive magmatism with enhanced mantle contributions at ca. 120–110 Ma. Two Jurassic–Cretaceous magmatic arcs are identified from the Caima–Duobuza–Rongma–Kangqiong–Amdo magmatic belt in the western Qiangtang Terrane and from the Along Tso–Yanhu–Daguo–Baingoin–Daru Tso magmatic belt in the northern Lhasa Terrane. These two magmatic arcs reflect northward and southward subduction of the Bangong Ocean lithosphere, respectively. Available multidisciplinary data reconcile that the Bangong Ocean may have closed during the Late Jurassic–Early Cretaceous (most likely ca. 140–130 Ma) through arc-arc "soft" collision rather than continent-continent "hard" collision. Subduction zone retreat associated with convergence beneath the Lhasa Terrane may have driven its rifting and separation from the northern margin of Gondwana leading to its accretion within Asia.

Keywords: Multidisciplinary data; Divergent double subduction; Bangong Ocean; "soft" Lhasa–Qiangtang collision; central Tibet

1. Introduction

The Wilson cycle involves the opening and closing of ocean basins and its recognition in the rock record provides a clear manifestation of the process of plate tectonics (e.g., Wilson, 1966; Dewey and Spall, 1975). Closure of ocean basins during the latter stages of the Wilson cycle involves the subduction of oceanic lithosphere and results in arc-continent or continent-continent collision. Two distinct geodynamic frameworks have been proposed for the closure of ocean basins (cf. Frisch et al., 2011). The first involves single-sided oceanic subduction leading to the development of a single magmatic arc on the overriding plate, subduction of the passive continental margin on the down-going plate, and development of large-scale fold and thrust structures and associated high-grade metamorphism in the collision zone. This pattern is exemplified by the Alpine-Himalayan orogen (cf. Sengör, 1987; Yin and Harrison, 2000; Leech et al., 2005). The second mechanism of ocean basin closure involves divergent double-sided oceanic subduction without significant subduction of the opposing continental blocks and leads to the development of two magmatic arcs on the opposing overriding plates, extensional basins, and generally low-grade metamorphism, as well as extensive long-lived granitoid magmatism with a mantle isotopic signature within the collision zone that postdates ocean closure (Soesoo et al., 1997). The modern Molucca Sea in eastern Indonesia (cf. Hinschberger et al., 2005) and the Paleozoic Solonker suture in central Asian Orogenic Belt (Xiao et al., 2003; Eizenhöfer et al., 2014, 2015a, 2015b) are

examples of this second mechanism. The distinct tectonic, metamorphic, and petrological consequences of single versus double divergent subduction zones during ocean basin closure (Soesoo et al., 1997; Zhao, 2015) provide a set of testable relationships for evaluating suture zones juxtaposing continental blocks in the geological record. The focus of this paper is to critically evaluate these features for differentiating the assembly of the Lhasa and Qiangtang terranes and intervening Bangong suture in central Tibet, which is ascribed to the Mesozoic closure of the Tethyan Bangong Ocean.

The existence of the Bangong Ocean is inferred from the presence of extensive dismembered ophiolitic fragments within the Bangong suture zone, which separates the Gondwana-derived Qiangtang and Lhasa terranes in central Tibet (Fig. 1a) (cf. Yin and Harrison, 2000; Zhu et al., 2013). The suture zone and its relationships with the bounding terranes have been highlighted as providing an important record of breakup, drift and accretion-related tectonism, magmatism, sedimentation, and metamorphism associated with the fragmentation of Gondwana's northern margin and subsequent assembly of the dispersed terranes into Asia. However, the details of the assembly history of the Bangong oceanic lithosphere including subduction polarity and timing of ocean closure remain in dispute. For example, the predominant view is that the ocean was subducted northward beneath the Qiangtang Terrane (Allègre et al., 1984; Yin and Harrison, 2000; Guynn et al., 2006; Kapp et al., 2007; Zhang et al., 2012a). Alternatively, some have argued for a

divergent double-sided subduction zone involving both northward subduction beneath the Qiangtang Terrane and southward subduction beneath the Lhasa Terrane (Pan et al., 2012; Zhu et al., 2013; Deng et al., 2014). Estimates for the time of closure of the Bangong Ocean range from the Middle Jurassic to Late Cretaceous (cf. Pan et al., 1983, 2012; Yin and Harrison, 2000; Kapp et al., 2007; Zhu et al., 2009, 2011, 2013; Zhang et al., 2012a; Fan et al., 2014).

In this paper, we integrate our new geochronological and geochemical data (see Tables S1–S3) with available information from the Bangong suture zone and show that the records of magmatism, sedimentation, and metamorphism are consistent with divergent double-sided subduction and associated mantle dynamics (e.g., Soesoo et al., 1997). This synthesis corroborates the southward subduction of Bangong Ocean lithosphere beneath the Lhasa Terrane and argues that this subduction is analogous to the westward subduction of the Pacific lithosphere that led to the development of back-arc basins in the western Pacific (Schellart et al., 2006; Cawood et al., 2009; Niu, 2014), providing a good example to evaluate mantle geodynamics operating during Gondwana dispersion and Asian accretion.

2. Geological record within the Bangong suture and adjacent regions

In central Tibet, the Bangong suture zone separates the Qiangtang Terrane to the north and the Lhasa Terrane to the south (Fig. 1a) (Yin and Harrison, 2000; Zhu et al., 2013). Based on the differences in basement rock and sedimentary cover, the

Lhasa Terrane is divided into northern, central, and southern subterranes, separated by the Shiquan River–Nam Tso Mélange Zone (SNMZ) and Luobadui–Milashan Fault (LMF), respectively (Zhu et al., 2011). The Qiangtang Terrane is divided into eastern and western subterranes separated by the Longmu Tso–Shuanghu suture zone (LSSZ) (Fig. 1a) (cf. Zhu et al., 2013). To evaluate the closure history of the Tethyan Bangong Ocean, this paper focuses on the Jurassic–Cretaceous sedimentary, metamorphic, and magmatic records of rock units and their relations within the Bangong suture zone and adjacent regions of the Lhasa and Qiangtang terranes, which are defined here as the Lhasa-Qiangtang collision zone (Figs. 1b and 2).

2.1. Lithostratigraphy

The Jurassic rock units in the northern Lhasa subterrane include sandstones with interstratified volcanic rocks (Jienu Group) (Fig. 1b), flysch sediments (Lagongtang Formation), and limestones (Rila Formation) (Fig. 2) (cf. Pan et al., 2004; Wang et al., 2013). These units are overlain by Lower Cretaceous volcano-sedimentary units (e.g., Qushenla and Duoni formations) (Zhu et al., 2006a) and younger limestones (Langshan Formation) and are intruded by varying-sized plutons (including the large Baingoin and Along Tso batholiths) (Fig. 2) (Xu et al., 1985; Haider et al., 2013). In the western Qiangtang subterrane a continuous Lower Jurassic succession is present (cf. Raterman et al., 2014), which contrasts with the northern Lhasa subterrane where rock units of this age are lacking. These units consist mainly of sandstones

and limestones along with some Upper Jurassic volcanic rocks (Amdo Formation) (Bai et al., 2005; Sun, 2005) and are intruded by 170–150 Ma granitoids (Fig. 2). Subsequent units include Lower Cretaceous conglomerates, sandstones, and limestones (Ouli and Dongqiao formations), and volcanic rocks (Meiriqiecuo Formation), lying unconformably on the Jurassic units (cf. Sun, 2005; Wang et al., 2013). The Jurassic to Lower Cretaceous units in the northern Lhasa and western Qiangtang subterranes are unconformably overlain by the Upper Cretaceous terrestrial molasse of the Jingzhushan and Abushan formations, respectively (Fig. 2) (Pan et al., 2004; Li et al., 2013a; Wang et al., 2013). Some units (e.g., Amdo, Dongqiao, and Qushenla formations) in the northern Lhasa and western Qiangtang subterranes extend into the Bangong suture zone (Fig. 2), which also includes the Muggargangri Group and Shamuluo Formation (Fig. 1b).

The Muggargangri Group consists mainly of interstratified sandstone, siltstone, and shale along with rare limestone, with the latter units possibly tectonically interleaved (Fig. 1b) (Wen, 1979; Cheng and Xu, 1986; Xia and Liu, 1997; Wang et al., 2013). The group is mainly Early to Middle Jurassic in age (Pan et al., 2004; Wang et al., 2013) but locally ranges into the Early Cretaceous (Kapp et al., 2007) (Fig. 2). This group has undergone extensive tectonic disruption and contains abundant ophiolitic fragments, and is generally interpreted as an accretionary complex (Pan et al., 2004; Duan et al., 2013; Wang et al., 2013). Equivalent units of the Muggargangri Group extend into the southern portion of the western

Qiangtang subterrane in the vicinity of Duobuza (Fig. 1b) (Duan et al., 2013) and into the northern edge of the Lhasa Terrane in the vicinity of Daru Tso (i.e. the Xihu Group) (Xia and Liu, 1997; Wang et al., 2013) (Fig. 1b).

The accretionary complex and associated ophiolitic fragments are unconformably overlain by the Shamuluo Formation (Fig. 2) that is exposed discontinuously within the Bangong suture zone (Fig. 1b). This formation consists of sandstone and siltstone interbedded with shale and fossil-rich limestone that yielded a Late Jurassic to Early Cretaceous age (Xia and Liu, 1997; Pan et al., 2004; Zhang et al., 2004; Wang et al., 2013). These Jurassic-Cretaceous units are intensely deformed and locally exhibit tight upright to overturned folds (Allègre et al., 1984; Yin et al., 1988; Yin and Harrison, 2000; Pan et al., 2004; Kapp et al., 2007; Wang et al., 2013; Volkmer et al., 2014). The youngest age group (ca. 210 Ma) of detrital zircons from sandstones of the Muggargangri Group north of Geize is consistent with derivation from the Qiangtang Terrane (Zeng et al., 2015).

In the western Bangong suture zone northwest of the Along Tso, the Shamuluo Formation extends onto the northern edge of the Lhasa Terrane (Fig. 1b) and is unconformably overlain by the Lower Cretaceous Qushenla Formation (Fig. 2). The Qushenla Formation in the northern Lhasa subterrane is dominated by volcanic rocks and is distributed from Along Tso–Yanhu in the west (referred to as the Yanhu volcanic rocks) to NW Baingoin (Fig. 1b). Subsequent sedimentation is characterized by the Aptian-Albian shallow marine limestone of the Langshan Formation (Fig. 2),

which is regionally exposed in the northern (Fig. 1b) and central Lhasa subterranes (Yin et al., 1988; Pan et al., 2004; Zhang et al., 2004; Kapp et al., 2005, 2007; Wang et al., 2013; Volkmer et al., 2014). Time-equivalent limestone is reported in the upper Dongqiao Formation in the vicinity of Dongqiao (Fig. 1b) within the Bangong suture zone (Wang and Dong, 1984; Zheng et al., 2003) and north of Amdo on the southern edge of the western Qiangtang subterrane (Bai et al., 2005; Sun, 2005) (Fig. 1b).

2.2. Metamorphism

Regional metamorphism within the Bangong suture zone was initially inferred to have occurred at ca. 171 Ma based on a lower intercept U-Pb age of discordant zircons and sphenes from the Amdo gneiss (Xu et al., 1985; Harris et al., 1988a). Subsequent study on the gneiss identified 185–170 Ma amphibolite-facies metamorphism on the basis of hornblende Ar-Ar dating and sphene U-Pb dating (Guynn et al., 2006), which was also verified by zircon U-Pb dating (Guynn et al., 2013). Recently, high-pressure granulite-facies metamorphism at ca. 190–180 Ma was documented from the Amdo metaigneous and metasedimentary rocks by zircon U-Pb dating (Zhang et al., 2010, 2012b, 2014a). Approximately coeval metamorphism may have occurred at Basu located ca. 400 km southeast of (Zhang et al., 2008) and at Dong Tso located ca. 700 km west of the Amdo gneiss (Wang et al., 2008) (Fig. 1b). All these geochronological data indicate metamorphism within

the Bangong suture zone occurred in the Early-Middle Jurassic (see Cohen et al., 2014 for time scale). On a regional scale, there is no isotopic age data for Early Cretaceous metamorphism of the Jurassic accretionary complex and other sedimentary units, and from the Jurassic ophiolitic fragments within the Bangong suture zone, which only include greenschist facies metamorphic mineral assemblages (Girardeau et al., 1984; Kapp et al., 2005; Sun, 2010). This contrasts with the India-Asia continental collision zone, where early Cenozoic high-grade metamorphic rocks that formed in response to this collision are locally present (cf. Leech et al., 2005; Donaldson et al., 2013).

2.3. Magmatic arc on the western Qiangtang subterrane

Early research in the western Qiangtang subterrane did not recognize any evidence for arc magmatism (cf. Pan et al., 1983; Allègre et al., 1984; Dewey et al., 1988). This contrasts with structural evidence for southward vergence of Cretaceous thrusts and the southward obduction of ophiolitic fragments onto the northern Lhasa subterrane, which was related to northward subduction beneath the Qiangtang Terrane (Girardeau et al., 1984; Kapp et al., 2003). The identification of 185–170 Ma granitoids (Fig. 2) in the Amdo microcontinent, which is interpreted to represent a “missing” Jurassic continental arc along the western Qiangtang subterrane, provides evidence for northward subduction (Guynn et al., 2006). More recent evidence for a continental arc along this subterrane include the Jurassic magmatism

from Caima-Duobuza-Qingcaoshan-Liqunshan in the west (170–150 Ma) (Kapp et al., 2005; Li et al., 2014a, 2014b, 2015a; Liu et al., 2014), from Rongma (ca. 150 Ma; Ran et al., 2015) and Kangqiong (ca. 148 Ma; Li et al., 2015c) in the center, and from the Upper Jurassic Amdo Formation in the east (Sun, 2005) (Fig. 1b).

The 170–150 Ma magmatism in the west (Figs. 1b and 2) is characterized by the presence of coeval calc-alkaline and highly fractionated I-type granitoids with mafic enclaves showing high-Nb and low Zr/Y geochemical signatures, indicative of continental arc magmatism associated with a MASH process (melting, assimilation, storage, and homogenization) above a subduction zone (Li et al., 2014a, 2014b). These Jurassic granitoids show more negative zircon $\varepsilon_{Hf}(t)$ values inboard (i.e., continentward) from Duobuza–Qingcaoshan to Liqunshan (Fig. 3a). This relationship is similar to that from the Gangdese arc in southern Tibet, which results from the northward subduction of the Yarlung-Zangbo oceanic lithosphere (cf. Zhu et al., 2011). This similarity further corroborates the presence of a continental arc during the Mid-Late Jurassic. To the east in Kangqiong (Fig. 1b), the granitoids show adakitic geochemical signatures with high Mg# (58–53), which are inferred to be derived from the partial melting of the subducting Bangong Ocean lithosphere (MORB + sediment) and subsequently hybridized by peridotite in the mantle wedge (Li et al., 2015c). To the north of Dongqiao, the volcanic rocks (including abundant volcaniclastic rocks) of the Amdo Formation (Fig. 1b) show a wide compositional spectrum from basalt to rhyolite but are dominated by andesite (Sun, 2005). Such

rock association, together with the high-Mg adakitic signature (Mg# = 62) of the andesite and the low Zr/Y (2.1–3.0) ratios of the basalts, indicate a convergent margin setting rather than continental extensional setting (Pearce and Norry, 1979) for their generation. These geochronological and geochemical data corroborate the presence of a Jurassic continental arc extending ca. 1100 km along the length of the western Qiangtang subterrane. Nevertheless, it should be noted that this arc (170–150 Ma) is likely younger than the arc proposed by Guynn et al. (2006) on the basis of the 185–170 Ma granitoids from Amdo.

In addition to the Jurassic magmatism, abundant Early Cretaceous magmatic rocks are also identified in the western Qiangtang subterrane (cf. Kapp et al., 2005, 2007; Liu et al., 2012; Li et al., 2013b, 2014a, 2015a) as exemplified mainly by the granitoids from Duobuza and the volcanic rocks from the Meiriqiecuo Formation (Figs. 1b and 2). The Duobuza granitoids are interpreted to link with the giant Duobuza porphyry Cu–Au deposit (cf. Li et al., 2013b, 2014a, 2015a). These rocks consist of 125–115 Ma diorite and granodiorite and show positive zircon $\varepsilon_{Hf}(t)$ values (+1 to +10; Fig. 3a) (Li et al., 2013b, 2014a, 2015a). The Meiriqiecuo volcanic rocks mainly occur in Duobuza and Rena Tso (Fig. 1b) and are dated at 124–105 Ma (Liu et al., 2012; Fan et al., 2015; Li et al., 2015a). Bimodal volcanic suites with different ages are reported from Duobuza (ca. 120 Ma; Fan et al., 2015) and Rena Tso (ca. 110 Ma; Liu et al., 2012). All available geochemical data indicate that the Meiriqiecuo volcanic rocks are exclusively high-K calc-alkaline or shoshonitic (Fig.

3b). Generally, the 125–105 Ma magmatism is interpreted as having formed in a magmatic arc as a result of the northward subduction of Bangong Ocean lithosphere beneath the Qiangtang Terrane (cf. Li et al., 2013b, 2014a, 2015a; Fan et al., 2015).

Early Cretaceous granitoids from both Qingcaoshan and Liqunshan show similar zircon $\varepsilon_{Hf}(t)$ values, while the coeval and younger Duobuza granitoids (120–104 Ma) display enhanced zircon $\varepsilon_{Hf}(t)$ values compared, to those of the Jurassic granitoids from each locality (Fig. 3a). Given the nature of a continental arc with ancient basement as indicated by the negative zircon $\varepsilon_{Hf}(t)$ values of the Jurassic granitoids, this difference points to an increased contribution of a mantle component (depleted asthenosphere- or enriched mantle wedge- or subcontinental lithospheric mantle-derived melt) in the generation of the Cretaceous Duobuza granitoids (120–104 Ma).

2.4. Magmatic arc on the northern Lhasa subterrane

Magmatic rocks are well documented from the northern Lhasa subterrane in central Tibet (cf. Pan et al., 1983; Allègre et al., 1984; Xu et al., 1985; Coulon et al., 1986; Harris et al., 1988b, 1990; Pearce and Mei, 1988), resulting in a hypothesis involving southward subduction of the Bangong Ocean lithosphere (cf. Pan et al., 1983; Allègre et al., 1984). The rocks are best exposed in the northern Lhasa subterrane. They include the Along Tso Batholith and Yanhu volcanic rocks in the west, the Baingoin Batholith in the east (Figs. 1b and 2), as well as other Jurassic-

Cretaceous volcano-sedimentary strata mostly distributed in the east (Fig. 2) (cf. Pan et al., 2004; Wang et al., 2013).

The Along Tso Batholith (Fig. 1b) is composed largely of granodiorite intruded by mafic dykes (Fig. 1c), dioritic enclaves and plutons, and monzogranites, showing a rock association similar to the Gangdese Batholith in the southern Lhasa subterrane (cf. Zhu et al., 2011, 2013). Zircon U-Pb age results suggest that the mafic dykes were emplaced at ca. 120 Ma (Fig. S1) (Table S1), while the granitoids (including granodiorite, dioritic enclave and intrusion, and monzogranite) were emplaced between ca. 120 and 110 Ma (Zhu et al., 2011; Sui et al., 2013). Although these rocks are inferred to be subduction-related (cf. Pan et al., 1983, 2012), there is no convincing geochemical evidence for this inference.

The Baingoin Batholith comprises two-mica tourmaline monzogranite intruded by ultrabasic dykes (Fig. 1d), granodiorite with dioritic enclaves that contains quartz xenocrysts (Fig. 1e), quartz diorite, tonalite, and syenogranite (Xu et al., 1985; Harris et al., 1990). Three monazites from a granite within the batholith yielded a mean U-Pb age of 121 ± 2 Ma, which was taken to represent its time of emplacement (Xu et al., 1985). Available new zircon U-Pb age data indicate emplacement ages ranging from 139 Ma to 110 Ma (Haider et al., 2013; Volkmer et al., 2014; this study). Magma chemistry changes through time (Zhu et al., 2012) as exemplified by the zircon $\varepsilon_{Hf}(t)$ values decreasing from ca. 132 Ma to ca. 120 Ma but increasing at 118–110 Ma (Fig. 3c) (Table S2).

The age of the Baingoin Batholith (Xu et al., 1985; Harris et al., 1990) (Fig. 3c) overlaps the timing of northward subduction of Neo-Tethyan Ocean lithosphere beneath the southern margin of the Lhasa Terrane (cf. Zhu et al., 2011, 2013). However, this is unlikely to be the geodynamic driver as the batholith was some 600 km from the southern margin (cf. Kapp et al., 2007; Leier et al., 2007) which would require low angle subduction (Coulon et al., 1986; Zhang et al., 2004; Kapp et al., 2005, 2007) that could not then account for coeval calc-alkaline magmatism along the terrane's southern margin (cf. Zhu et al., 2011, 2013). The increasing zircon $\varepsilon_{Hf}(t)$ values of the 118–110 Ma granitoids (Fig. 3c) and the presence of dioritic enclaves and ultrabasic dykes (Fig. 1d) point to enhanced mantle contributions, which are unlikely to be explained by the hypothesis arguing for crustal anatexis in relation to intra-block thrusting resulting from the Lhasa-Qiangtang collision (Xu et al., 1985). Instead, the positive zircon $\varepsilon_{Hf}(t)$ values of the 132 ± 2 Ma granitoids indicate that their parent magmas most likely originated from the partial melting of juvenile crust. This, together with the apparent southward (i.e., continentward) decrease in zircon $\varepsilon_{Hf}(t)$ values of the Mesozoic–early Tertiary rocks from the four north–south traverses across the Lhasa Terrane (Zhu et al., 2011), indicate that the Bangong Ocean lithosphere likely subducted southward beneath the Lhasa Terrane.

The Yanhu volcanic rocks (Figs. 1b and 2) provide additional evidence for the southward subduction of the Bangong Ocean lithosphere beneath the northern Lhasa subterrane. These rocks consist primarily of andesite with minor basalt and

rhyolite (Fig. 3b), forming a bimodal volcanic suite in places (Fig. 1f) (Sui et al., 2013). Zircon U-Pb age (Zhu et al., 2011) and whole-rock geochemical data of these rocks reveal a distinct compositional variation with time, i.e. from calc-alkaline (131–120 Ma) to high-K calc-alkaline and shoshonitic (116–110 Ma) (Fig. 3b). Such variation most likely reflects a change in tectonic affinity from arc-related (131–120 Ma) to rift-related (116–110 Ma) as indicated by their clinopyroxene chemistry (Fig. 3d) (Table S3), which provides a diagnostic means of establishing the tectonomagmatic affinity of host rocks (Loucks, 1990).

Magmatic arc activity along the northern Lhasa subterranes is probably as old as mid-Jurassic based on the presence of the ca. 164 Ma high-Mg andesites recently identified from the eastern bank of Daru Tso (Li et al., 2015d). These rocks display high MgO (5.04–7.43 wt.%), Mg# (63–70), and low Y (12–17 ppm) with negative zircon $\varepsilon_{Hf}(t)$ (–8.5 to –6.7) (Li et al., 2015d), indicative of derivation by partial melting of subducting ocean lithosphere with sediments followed by hybridization of peridotite in the mantle wedge. Coeval volcanic rocks, commonly referred to as the Jienu Group of Mid-Late Jurassic age (Fig. 2) (cf. Yin et al., 1988; Pan et al., 2004; Wang et al., 2013), are discontinuously distributed in the northern Lhasa subterrane at Rutog in the west, Oma in the center, and Daru Tso in the east (Fig. 1b). Unfortunately no geochronological and geochemical data are available for the Jienu Group volcanic rocks at either Rutog or Oma. However, given the stratigraphic comparison and the exposed locations of these Jurassic volcanic rocks (including the

ca. 164 Ma Daru Tso high-Mg andesite), their generation is attributed to the southward subduction of the Bangong Ocean lithosphere beneath the Lhasa Terrane.

2.5. Early Cretaceous (120–110 Ma) mafic magmatism within the Bangong suture zone

Mafic magmatism of late Early Cretaceous age (120–110 Ma) within the Bangong suture zone occurs at Tarenben and Duoma (Zhu et al., 2006), Zhonggang (Fan et al., 2014), and Julu (Liu et al., 2014) (Figs. 1b and 2). The basalts from Duoma and Tarenben occur as pillow lavas interbedded with bioclastic limestone and purplish red chert and yield zircon U-Pb age of ca. 108 Ma (Zhu et al., 2006). The Zhonggang basalts are interbedded with limestone and are intruded by cogenetic gabbro, which is dated by U-Pb zircon at ca. 116 Ma (Fan et al., 2014). The Julu basalts occur as pillow lavas intercalated with radiolarian chert and are likely emplaced at ca. 104 Ma on the basis of a U-Pb zircon age on cogenetic gabbro (Liu et al., 2014). Other occurrences of possible Early Cretaceous mafic magmatism within the Bangong suture zone (Zhang et al., 2014b) are not considered here because of the absence of age data (e.g., Riganpei Tso and Pudu Tso) or an inconsistency between the determined $^{40}Ar/^{39}Ar$ age (Zhang et al., 2014b) and sedimentary records (e.g., Penghu; Wang et al., 2013).

Available geochemical data indicate that the Early Cretaceous mafic magmatism within the Bangong suture zone consists of ocean island basalt (OIB)-like rocks that

display positive Nb-Ta anomalies, as seen in Tarenben and Duoma (Zhu et al., 2006) and Zhonggang (Fan et al., 2014), and arc-like rocks that exhibit negative Nb-Ta anomalies as exemplified by the Julu basalts (Liu et al., 2014). Zr/Y and Nb/Y ratios, expressed as δNb values [= log (Nb/Y) + 1.74 – 1.92 × log (Zr/Y)], provide information on the source of the basalts (Fitton et al., 1997). The high Zr/Y ratios and positive δNb values of the OIB-like rocks suggest a deep-mantle source (Fig. 4) (Fitton et al., 1997), whereas the low Zr/Y ratios and negative to positive δNb values of the arc-like rocks point to a mixed mantle source involving a shallow N-MORB source (δNb < 0) and a deep depleted source (δNb > 0). Such mixed characteristic of magma source region is analogous to that documented by the Iron King volcanic rocks from west-central Arizona involving arc and oceanic plateau components (Condie et al., 2002).

3. Discussion

3.1. Reevaluation on the timing of the Lhasa-Qiangtang collision

Three hypotheses have been proposed for the timing of the Lhasa-Qiangtang collision.

Hypothesis I: Collision initiates in the Middle Jurassic and ends in the Late Cretaceous. Changing sedimentary environments along the Bangong suture zone, led Pan et al. (1983) to propose that collision between the Lhasa and Qiangtang terranes was diachronous commencing in the Middle Jurassic in the east and

terminating in the Late Cretaceous in the west. Xu et al. (1985) argued that the Lhasa-Qiangtang collision probably occurred in the Middle Jurassic on the basis of metamorphism of the Amdo gneiss at ca. 171 Ma. However, subsequent work on the amphibolite-facies to granulite-facies metamorphism of the Amdo gneiss and Basu eclogite indicates an Early Jurassic age (190–170 Ma), which is interpreted to represent the accretion between micro-continents (e.g., Amdo and Basu) within the Bangong Ocean and the Qiangtang Terrane (Guynn et al., 2006, 2013; Zhang et al., 2008, 2014a).

Hypothesis II: Collision terminates in the Late Cretaceous. The presence of 120–108 Ma OIB-type basaltic rocks and interbedded bioclastic limestones within the Bangong suture zone (Figs. 1b and 2) has been interpreted to indicate the presence of oceanic islands, and thus oceanic crust, within the Bangong suture zone (Zhu et al., 2006; Fan et al., 2014; Liu et al., 2014; Zhang et al., 2014a). However, this hypothesis is inconsistent with paleomagnetic data in which the southern margin of the Lhasa Terrane remained at latitude ~20 ± 4°N during ca. 110–50 Ma (Lipper et al., 2014). Given that the Lhasa Terrane was probably approximately 600 km wide in the Early Cretaceous (Kapp et al., 2007; Leier et al., 2007) this would imply a paleolatitude for the northern margin of ca. ~26 ± 4°N. Such a paleolatitude is virtually indistinguishable from that of the southern margin of the Qiangtang Terrane as indicated by the new paleomagnetic data (29.3 ± 5.7°N) of the ca. 110–104 Ma volcanic rocks from NE Gerze (Chen et al., 2015). Although the errors

on the paleomagnetic data are large enough that may indicate the presence of an ocean basin between the Lhasa Terrane and Qiangtang Terrane at this time, the results of stratigraphic and structural studies (cf. Kapp et al., 2007; Raterman et al., 2014) and mantle dynamics described below allow us to argue that the Lhasa Terrane may have already collided with the Qiangtang Terrane prior to ca. 110 Ma.

Hypothesis III: Collision occurs during the Late Jurassic to Early Cretaceous. This hypothesis was based on the single zircon U-Pb ages of 140–120 Ma for the Amdo granite (Xu et al., 1985), which was interpreted as having derived from the anatexis of a Proterozoic crust in a collisional environment (Allègre et al., 1984; Dewey et al., 1988). This interpretation for the Amdo granite formed the basis for the model of Yin and Harrison (2000), who argued that the Lhasa-Qiangtang collision took place in the late Jurassic near Amdo (Long. 91°E) and in the middle Cretaceous near Shiquan River (Long. 80°E). Additional evidence for this hypothesis comes from the stratigraphic and structural studies along the Bangong suture zone. Ophiolites south of Tsige Dartso are unconformably overlain by the Lower Cretaceous Dongqiao Formation, which consists of a lower succession of ophiolitic-derived sandstone and conglomerate (Fig. 2) and an upper bioclastic limestone (Aptian–Albian; 125–100 Ma) (Wang and Dong, 1984; Yin et al., 1988; Zheng et al., 2003). East of Dongqiao, around Amdo, the lowermost Dongqiao Formation conglomerate is unconformable on fossiliferous strata with ages of early Cretaceous (143–131 Ma; Sun, 2005). To the west of Dongqiao in the Nyima basin,

geological mapping and geochronological data indicated that this basin underwent major deformation and denudation resulting in it evolving from marine to nonmarine environments between ca. 125 Ma and ca. 118 Ma (Kapp et al., 2007). Further to the west in Domar within the western Qiangtang subterrane (Fig. 1b), structural mapping and detrital zircon U-Pb dating identified a significant Late Jurassic–Early Cretaceous shortening rather than significant Cenozoic shortening in response to the India-Asia collision (Raterman et al., 2014). All these observations are interpreted to be associated with the Lhasa-Qiangtang collision during the Late Jurassic to Early Cretaceous (Wang and Dong, 1984; Yin et al., 1988; Zheng et al., 2003; Sun, 2005; Kapp et al., 2007; Raterman et al., 2014). On the other hand, the well-developed Upper Cretaceous terrestrial molasse sedimentary rocks, such as the Jingzhushan Formation on the northern Lhasa and the Abushan Formation on the western Qiangtang subterranes Fig. 1b), suggest that the two terranes had collided by this time.

In summary, the lithotectonic evidence for deformation and crustal thickening, evidenced by angular unconformities and accumulation of non-marine successions in the Bangong suture zone in the mid-Cretaceous, as well as the scarcity of 140–130 Ma magmatic in the western Qiangtang subterrane (Li et al., 2014a), and the presence of ca. 114 Ma anorogenic felsic (A2-type) rocks that point to a postcollisional setting (Eby, 1992) identified in the northern Lhasa subterrane (Chen

et al., 2014), support Lhasa-Qiangtang collision taking place in the Late Jurassic to Early Cretaceous, most likely 140–130 Ma.

3.2. A divergent double-sided subduction model for the closure of the Bangong Ocean

The closure of the Bangong Ocean is widely ascribed to the continental collision between the Lhasa and Qiangtang terranes (Kapp et al., 2003, 2005, 2007; Zhang et al., 2004, 2012a; Volkmer et al., 2014). This model appears to be supported by the similarities of structural styles between the northern Lhasa and Tethyan Himalayan thrust belts (Raterman et al., 2014), both of which represent passive margins on the lower subducting plate of a collision zone. However, Early Cretaceous magmatism is extensive in the northern Lhasa subterrane (Figs. 1b and 2), which is in contrast to the Tethyan Himalaya where Cenozoic magmatism is limited to small leucogranite bodies. This difference was first noted by Harris et al. (1990), who suggested that the temperatures required for the origin of the extensive magmatism in the northern Lhasa subterrane cannot result from continental collision between two major lithospheric blocks, as in the Tertiary evolution of the Himalayas, but can better be described as docking between terranes. High-temperature magma generation during the Early Cretaceous in the northern Lhasa subterrane has been corroborated by the identification of ca. 114 Ma anorogenic (A2-type) magmatism at Daguo (Fig. 1b) (Chen et al., 2014), the

increase in mantle contributions at 120–110 Ma in the Duobuza granitoids (Fig. 3a) and at 118–110 Ma in the Baingoin Batholith (Fig. 3c), and the subduction- to extension-related magmatism (131–110 Ma) at Yanhu (Fig. 3d). South-directed thrusting in the northern Lhasa subterrane has been related to subduction beneath the Qiangtang Terrane. However, the timing of thrusting ranges in age from Late Cretaceous to earliest Tertiary (cf. Murphy et al., 1997; Kapp et al., 2003, 2005, 2007; Volkmer et al., 2014), postdating the timing of final Lhasa-Qiangtang amalgamation. This means that such south-directed thrusting may have been strengthened by the northward subduction of the Neo-Tethyan Ocean lithosphere beneath the southern Lhasa subterrane and thus cannot be considered as a strong argument for the northward subduction of the Tethyan Bangong Ocean lithosphere beneath the Qiangtang Terrane.

The absence of the Early Cretaceous high-grade metamorphic rocks along the Bangong suture zone may be attributed to the low degrees of exhumation, analogous to absence of such rocks in parts of the Coast Mountains arc in western North America (Rusmore et al., 2005) and/or to the presence of a sedimentary cover as interpreted for the lack of Jurassic granitoids in places in the western Qiangtang subterrane (Guynn et al., 2006). However, these two possibilities are less likely because no Early Cretaceous high-grade metamorphic rocks have been documented along the entire Bangong suture zone despite the fact that (1) the sedimentary cover for the western Qiangtang subterrane is only ca. 3.5 km thick

(Haines et al., 2003) and (2) the Lhasa-Qiangtang collision zone experienced rapid exhumation from mid-crustal levels between 108 and 90 Ma (Kapp et al., 2007; Volkmer et al., 2014). Thus, the lack of Early Cretaceous high-grade metamorphic rocks most likely reflects the distinct character of the subduction-collision history rather than varying degrees of subsequent exhumation along the Bangong suture zone.

Given the presence of magmatic arc rocks on both the northern margin of the Lhasa Terrane and the southern margin of the Qiangtang Terrane, and the lack of Early Cretaceous high-grade metamorphic rocks in the Lhasa-Qiangtang collision zone, we suggest that the Bangong Ocean closed via divergent double-sided subduction resulting in soft collision of opposing arcs (Soesoo et al., 1997). We outline the following 4 stage model which accounts for available stratigraphic, structural, metamorphic and magmatic character of the region:

Stage A (> 140 Ma): Subduction of the Bangong Ocean lithosphere may have begun as early as the Middle Permian beneath the Lhasa Terrane, perhaps triggered by collision of the southern margin of the terrane with northern Australia (cf. Zhu et al., 2011, 2013). Subduction of the ocean beneath the western Qiangtang subterrane likely initiated in the Mid-Late Triassic triggered by the Western-Eastern Qiangtang collision (Zhu et al., 2013; Zeng et al., 2015). This was accompanied by the development of the Jurassic accretionary complex, including the Muggargangri Group that is associated with subduction underneath the Qiangtang Terrane and the

Xihu Group that is associated with subduction underneath the Lhasa Terrane (Fig. 5a). Spreading within the Bangong Ocean may have ceased in the Late Jurassic on the basis of OIB-type basaltic rocks and slab-derived dacitic adakites in the western Qiangtang subterrane (156 ± 2 Ma) which are interpreted to reflect oceanic ridge subduction (Li et al., 2015e). Arc-related magmatism at this stage was represented by the 170–150 Ma granitoids and Amdo Formation volcanic rocks in the western Qiangtang (Fig. 1b) and the ca. 165 Ma Jienu Group volcanic rocks (Li et al., 2015d) and coeval granitoids in the northern Lhasa subterrane (Fig. 5a).

Stage B (140–130 Ma): Continued divergent subduction ultimately leads to the closure of the Bangong Ocean (Fig. 5b). Consequently, the northern Lhasa and western Qiangtang subterranes were welded together through "soft" arc-arc collision. Coeval sedimentation and deformation led to complicated tectono-sedimentary relationships within the collision zone, as exemplified by the angular unconformities between the Shamuluo and Qushenla formations with their underlying strata (Fig. 2) (Yin et al., 1988; Zheng et al., 2003; Zhang et al., 2004; Kapp et al., 2005, 2007; Wang et al., 2013). Magmatism at this stage is weak or absent due to the termination of normal subduction (Soesoo et al., 1997) explaining the scarcity of magmatic rocks of 140–130 Ma in both the western Qiangtang and the northern Lhasa subterranes.

Stage C (130–120 Ma): The cold and dense Bangong oceanic lithosphere below the "soft" arc-arc collision zone ruptures and detaches due to gravitational instability

(Soesoo et al., 1997), resulting in the upwelling of materials from the mantle wedge. This rupture most likely occurs in the south of the collision zone (Fig. 5c), facilitating the decompression and dehydration melting of mantle wedge materials, producing calc-alkaline melts with arc signatures (Figs. 3b and 3d). This phase is represented by the 131–120 Ma Yanhu volcanic rocks and the ca. 120 Ma mafic dykes (Fig. 1) in the northern Lhasa subterrane and melting of juvenile crust and overlying sedimentary rocks that generated the 134–130 Ma metaluminous (with positive zircon $\varepsilon_{Hf}(t)$ values) and the 125–120 Ma peraluminous (with negative zircon $\varepsilon_{Hf}(t)$ values) granitoids (Fig. 3c) in the Baingoin Batholith. In the north of the collision zone, the oceanic lithosphere remains attached to the overlying sedimentary section (Fig. 5c), small-scale mantle flow provides limited convective heat (Magni et al., 2012), consequently producing minor magmatism as documented in the western Qiangtang subterrane at this stage.

Stage D (120–110 Ma): Continued sinking of the Bangong Ocean lithosphere leads to the rupture propagating from the south to the north, eventually resulting in its complete detachment from the overlying crust (Soesoo et al., 1997) and/or breakoff due to continued slab pull through mineral phase changes at depth producing excess negative buoyancy (Niu, 2014) (Fig. 5d). Such processes create a gap that is filled with upwelling hot asthenosphere, consequently resulting in partial melting of the asthenosphere and the overriding metasomatized lithosphere to produce mafic magmatism that continues for a few millions of years and induce

crustal (including overlying crust and sedimentary rocks) anatexis that can proceed over a considerably longer period (van de Zedde and Wortel, 2001). As a result, magmatism occurs throughout the collision zone (Figs. 1b and 5d) and displays a compositional diversity with variable enhanced mantle contributions, explaining the presence of the 120–104 Ma granitoids in Duobuza in the western Qiangtang subterrane (Fig. 3a) and the 118–110 Ma granitoids from the Baingoin Batholith in the northern Lhasa subterrane (Fig. 3c).

The divergent double subduction model explains the following features that characterize the Lhasa-Qiangtang collision zone: a) absence of Early Cretaceous high-grade metamorphic rocks of continental crust due to the detachment of the continental crust from dense oceanic lithosphere (Soesoo et al., 1997) preventing the deep subduction and accompanying metamorphism of the continental lithosphere; b) Aptian-Albian shallow-marine limestone sedimentation (including the Langshan and Dongqiao formations and their equivalent strata within the Bangong suture zone) representing accumulation in a syncontractional basin (Kapp et al., 2005, 2007; Leier et al., 2007) in which subsidence was driven by the sinking of the Bangong Ocean lithosphere (Soesoo et al., 1997; Zhao et al., 2015) rather than a back-arc extension basin related to low-angle northward subduction of the Neo-Tethyan ocean lithosphere (Zhang et al., 2004); c) ca. 120–110 Ma OIB- and arc-like rocks (Fig. 4) within the Bangong suture zone (Figs. 1b and 2) that were derived from the varying-degree decompression melting of asthenospheric materials

(Ferrari, 2004) enveloped by the inverted-U–shaped oceanic slab due to the breakoff of the Bangong Ocean lithosphere (Fig. 5d). The association of coeval limestones and OIB-like rocks that formed in this setting resemble ocean islands, but are not indicative of the presence of oceanic crust as previously interpreted (Zhu et al., 2006; Fan et al., 2014).

3.3. Broader implications

The observations and interpretations presented above show that the Bangong Ocean most likely experienced pre-Cretaceous double-sided subduction, which is analogous to the modern Pacific Ocean whose lithosphere displays an advancing subduction zone beneath the western South American plate resulting in the deformation of the overriding plate (corresponding to the Qiangtang Terrane) and retreating subduction zone beneath the eastern Australian and Eurasian plate causing the overriding plate to extend (corresponding to the Lhasa Terrane) (Schellart et al., 2006; Cawood et al., 2009; Niu, 2014). In particular, the northward retreat of the southward-dipping subduction zone may have driven the separation of the Lhasa Terrane from Gondwana margin during the Late Triassic (Sengör, 1979; Zhu et al., 2011, 2013; Pan et al., 2012; Metcalfe, 2013) and the development of back-arc basins represented by the Shiquan River-Nam Tso mélange zone during the Mid-Late Jurassic (Zhu et al., 2011, 2013; Pan et al., 2012). This is analogous to the eastward retreat of the western Pacific subduction zones that led

to the development of back-arc basins in the western Pacific (Schellart et al., 2006; Cawood et al., 2009; Niu, 2014), providing a reasonable geodynamic mechanism responsible for the Gondwana dispersion and Asian accretion.

This synthesis demonstrates that the Bangong Ocean may have closed through arc-arc "soft" collision driven by divergent double-sided subduction (Fig. 5) during the Early Cretaceous, analogous to the modern Molucca Sea lithosphere subduction in eastern Indonesia (Hinschberger et al., 2005). Unlike the continent-continent hard collision (e.g., the Tertiary India-Asia collision) that was followed by continental deep subduction (cf. Leech et al., 2005), such arc-arc "soft" collision was most likely accompanied by the detachment of dense oceanic lithosphere without the involvement of continental deep subduction (Soesoo et al., 1997; Zhao, 2015). Such detachment will result in the loss of a slab pull force from the descent of the normal subducting Bangong Ocean lithosphere, leading to the preservation of its overlying accretionary complex systems (e.g., the Muggargangri and Xihu Group) (Fig. 1b), oceanic plateaux or seamounts, and enclosed microcontinent (e.g., the Amdo microcontinent) that are too buoyant to subduct (cf. Niu et al., 2003; Cawood et al., 2009; Niu, 2014). This would explain the presence of the diffuse ophiolitic mélanges (> 100 km wide) from Amdo to Daru Tso (Fig. 1b) (Pearce and Mei, 1988; Pan et al., 2004; Wang et al., 2013) within the Lhasa-Qiangtang collision zone. "Soft" collision through double-sided subduction may be applicable to other accretionary

orogens with well-preserved accretionary complex and ophiolitic fragments (e.g., the Central Asian Orogenic Belt, Xiao et al., 2003).

Although closure of the Bangong Ocean by divergent double-sided subduction, accounts for the observed geological features of the Lhasa-Qiangtang collision zone in central Tibet, further data on the provenance of the Jurassic–Cretaceous sedimentary rocks within the Bangong suture zone and in the northern Lhasa subterrane are needed to establish if they were sourced from the arc on the western Qiangtang or the arc on the northern Lhasa subterranes. Also the nature and evolution of the Jurassic–Cretaceous Daru Tso–Nagqu basin needs to be resolved to determine if it was built on accretionary complex, ophiolite or continental crust.

4. Conclusions

(1) The Bangong Ocean lithosphere was most likely subducted northward beneath the Qiangtang Terrane and southward beneath the Lhasa Terrane, forming two Jurassic–Cretaceous magmatic arcs currently represented by the opposing Caima–Duobuza–Rongma–Kangqiong–North Amdo magmatic belt and the Along Tso–Yanhu–Daguo–Baingoin–Daru Tso magmatic belt, respectively.

(2) Extensive 120–110 Ma magmatism with enhanced mantle contributions occurs within the Lhasa-Qiangtang collision zone, and this zone only experienced low-grade greenschist-facies metamorphism rather than high-grade amphibolite- to granulite-facies metamorphism in the Early Cretaceous.

(3) The Bangong Ocean may have closed during the Late Jurassic–Early Cretaceous (most likely ca. 140–130 Ma) through arc-arc "soft" collision rather than continent-continent "hard" collision.

(4) The special geological features that characterize the Lhasa-Qiangtang collision zone are consistent with the divergent double-sided subduction of the Bangong Ocean lithosphere and associated distinct mantle dynamics.

Acknowledgements

This paper is dedicated to Prof. Guitang Pan for his outstanding contribution to the geology of the Qinghai-Tibet Plateau. This research was financially co-supported by the Strategic Priority Research Program (B) of the Chinese Academy of Sciences (XDB03010301), the National Key Project for Basic Research of China (2011CB403102 and 2015CB452604), the Chinese National Natural Science Foundation (41225006, 41472061, and 40973026), and the Specialized Research Fund for the Doctoral Program of Higher Education (20120022110001). We thank Xiu-Mian Hu, Yaoling Niu, Ya-Lin Li, Chengshan Wang, and Quan-Ru Geng for useful discussions and comments on this manuscript. We also thank two anonymous reviewers for their constructive reviews that improved the quality of this manuscript.

References

Allègre, C.J., Courtillot, V., Tapponnier, P., and other 32 co-authors, 1984. Structure and evolution of the Himalaya–Tibet orogenic belt. Nature 307, 17–22.

Bai, Z.D., Xu, D.B., Zhang, Zhang, X.J., Zhu, G.X., Sun, L.X., 2005. 1:250, 000 geological report of Amdo with geological map. China University of Geosciences, Beijing, 63–14 (unpublished, in Chinese).

Cawood, P.A., Kröner, A., Collins, W.J., Kusky, T.M., Mooney, W.D., Windley, B.F., 2009. Accretionary orogens through Earth history. Geological Society, London, Special Publications 318, 1–36.

Chen, W.W., Zhang, S.H., Ding, J.K., Zhang, J.H., Zhao, X.X., Zhu, L.D., Yang, W.G., Yang, T.S., Li, H.Y., Wu, H.C., 2015. Combined paleomagnetic and geochronological study on Cretaceous 1 strata of the Qiangtang terrane, central Tibet. Submitted to Gondwana Research, in revision.

Chen, Y., Zhu, D.C., Zhao, Z.D., Meng, F.Y., Wang, Q., Santosh, M., Wang, L.Q., Dong, G.C., Mo, X.X., 2014. Slab breakoff triggered ca. 113 Ma magmatism around Xainza area of the Lhasa Terrane, Tibet. Gondwana Research 26, 449–463.

Chen, Y.L., Zhang, K.Z., Gou, Y.D., Wen, J.H., 2005. 1:250, 000 geological report of Oma with geological map. Sichuan Institute of Geological Survey, Chengdu, 41–53 (unpublished, in Chinese).

Cheng, J., Xu, G., 1986. Geological Map of the Gaize Region with Report (scale 1:1,000,000). Chengdu, Tibetan Bureau of Geology and Mineral Resources, p. 1–369.

Cohen, K.M., Finney, S.C., Gibbard, P.L., Fan, J.X., 2014. The ICS International Chronostratigraphic Chart. Episodes 36, 199–204.

Condie, K.C., Frey, B., Kerrich, R., 2002. The 1.75-Ga Iron King Volcanics in west-central Arizona: A remnant of an accreted oceanic plateau derived from a mantle plume with a deep depleted component. Lithos 64, 49–62.

Coulon, C., Maluski, H., Bollinger, C., Wang, S., 1986. Mesozoic and Cenozoic volcanic rocks from central and southern Tibet: $^{39}Ar/^{40}Ar$ dating, petrological characteristics and geodynamical significance. Earth and Planetary Science Letters 79, 281–302.

Deng, J., Wang, Q.F., Li, G.J., Li, C.S., Wang, C.M., 2014. Tethys tectonic evolution and its bearing on the distribution of important mineral deposits in the Sanjiang region, SW China. Gondwana Research 26, 419–437.

Dewey, J.F., Shackleton, R.M., Chang, C.F., Sun, Y.Y., 1988. The Tectonic Evolution of the Tibetan Plateau. Philosophical Transactions of the Royal Society of London (Series A): Mathematical and Physical Sciences 327, 379–413.

Dewey, J.F., Spall, H., 1975. Pre-Mesozoic plate tectonics: How far back in Earth history can the Wilson Cycle be extended? Geology 3, 422–424.

Donaldson, D.G., Webb. A.A.G., Menold. C.A., Kylander-Clark, A.R.C., Hacker, B.R., 2013. Petrochronology of Himalayan ultrahigh-pressure eclogite. Geology 41, 835–838.

Duan, Z.M., Li, G.M., Zhang, H., Duan, Y.Y., 2013. The formation and its geologic significance of Late Triassic-Jurassic accretionary complexes and constraints on metallogenic and geological settings in Duolong porphyry copper gold ore concentration area, northern Bangong Co-Nujiang suture zone, Tibet. Geological Bulletin of China 32, 742–750 (in Chinese with English abstract).

Eby, G.N., 1992. Chemical subdivision of the A-type granitoids: Petrogenetic and tectonic implications. Geology 20, 641–644.

Eizenhöfer, P.R., Zhao, G.C., Zhang, J., Sun, M., 2014. Timing of final closure of the Paleo-Asian Ocean along the Solonker Suture Zone: constraints from the provenance analysis of detrital zircons from Permian sedimentary rocks. Tectonics 33, 441–463.

Eizenhöfer, P.R., Zhao, G.C., Zhang, J., Han, Y.G., Hou, W.Z., Liu, D.X., Wang, B., 2015a. Geochemical characteristics of the Permian basins and their provenances across the Solonker Suture Zone: Assessment of net crustal growth during the closure of the Palaeo-Asian Ocean. Lithos 224, 240–255.

Eizenhöfer, P.R., Zhao, G.C., Sun, M., Zhang, J., Han, Y.G., Hou, W.Z., 2015b. Geochronological and Hf isotopic variability of detrital zircons in Paleozoic strata

across the accretionary collision zone between the North China craton and Mongolian arcs and tectonic implications. GSA Bulletin, doi: 10.1130/B31175.1.

Fan, J.J., Li, C., Xie, C.M., Wang, M., 2014. Petrology, geochemistry, and geochronology of the Zhonggang ocean island, northern Tibet: Implications for the evolution of the Banggongco–Nujiang oceanic arm of the Neo-Tethys. International Geology Review 56, 1504–1520.

Fan, J.J., Li, C., Xie, C.M., Wang, M., Chen, J.W., 2015. Petrology and U–Pb zircon geochronology of bimodal volcanic rocks from the Maierze Group, northern Tibet: Constraints on the timing of closure of the Banggong–Nujiang Ocean. Lithos 227, 148–160.

Ferrari, L., 2004. Slab detachment control on mafic volcanic pulse and mantle heterogeneity in central Mexico. Geology 32, 77–80.

Fitton, J.G., Saunders, A.D., Norry, M.J., Hardarson, B.S., Taylor, R.N., 1997. Thermal and chemical structure of the Iceland plume. Earth and Planetary Science Letters 153, 197–208.

Frisch, W., Meschede, M., Blakey, R., 2011. Plate Tectonics: Continental drift and mountain building. Springer-Verlag Berlin Heidelberg, p. 149–158.

Girardeau, J., Marcoux, J., Allègre, C.J., Bassoullet, J.P., Tang, Y.K., Xiao, X.C, Zao, Y.G., Wang, X.B., 1984. Tectonic environment and geodynamic significance of the Neo-Cimmerian Donqiao ophiolite, Bangong-Nujiang suture zone, Tibet. Nature 307, 27–31.

Guynn, J., Tropper, P., Kapp, P., Gehrels, G.E., 2013. Metamorphism of the Amdo metamorphic complex, Tibet: Implications for the Jurassic tectonic evolution of the Bangong suture zone. Journal of Metamorphic Geology 31, 705–727.

Guynn, J.H., Kapp, P., Pullen, A., Gehrels, G.E., Heizler, M., Ding, L., 2006. Tibetan basement rocks near Amdo reveal "missing" Mesozoic tectonism along the Bangong suture, central Tibet. Geology 34, 505–508.

Haines, S.S., Klemperer, S.L., Brown, L., Guo, J.R., Mechie, J., Meissner, R., Ross, A., Zhao W.J., 2003. INDEPTH III seismic data: from surface observations to deep crustal processes in Tibet. Tectonics 22, 1001. doi: 10.1029/2001TC001305.

Harris, N.B.W., Holland, T.J.B., Tindle, A.G., 1988a. Metamorphic rocks of the 1985 Tibet Geotraverse, Lhasa to Golmud. Philosophical Transactions of the Royal Society of London Series A–Mathematical Physical and Engineering Sciences 327, 203–213.

Harris, N.B.W., Inger, S., Xu, R.H., 1990. Cretaceous plutonism in Central Tibet: An example of post-collision magmatism? Journal of Volcanology and Geothermal Research 44, 21–32.

Harris, N.B.W., Xu, R.H., Lewis, C.L., Jin, C.W., 1988b. Plutonic rocks of the 1985 Tibet Geotraverse, Lhasa to Golmud. Philosophical transactions of the Royal Society of London. Series A, mathematical and physical. Sciences 327 (1594), 145–168.

Hastie, A.R., Kerr, A.C., Pearce, J.A., Mitchell, S.F., 2007. Classification of altered volcanic island arc rocks using immobile trace elements: development of the Th–Co discrimination diagram. Journal of Petrology 48, 2341–2357.

Hinschberger, F., Malod, J.A., Réhault, J.P., Villeneuve, M., Royer, J.Y., Burhanuddin, S., 2005. Late Cenozoic geodynamic evolution of eastern Indonesia. Tectonophysics 404, 91–118.

Kapp, P., DeCelles, P.G., Gehrels, G.E., Heizler, M., Ding, L., 2007. Geological records of the Lhasa–Qiangtang and Indo-Asian collisions in the Nima area of central Tibet. Geological Society of America Bulletin 119, 917–932.

Kapp, P., Yin, A., Harrison, T.M., Ding, L., 2005. Cretaceous–Tertiary shortening, basin development, and volcanism in central Tibet. GSA Bulletin 117, 865–878.

Leech, M.L., Singh, S., Jain, A.K., Klemperer, S.L., Manichavasgam, R.M., 2005. The onset of India-Asia continental collision: Early, steep subduction required by the timing of UHP metamorphism in the western Himalaya. Earth and Planetary Science Letters 234, 83–97.

Leier, A.L., Decelles, P.G., Kapp, P., Gehrels, G.E., 2007. Lower Cretaceous strata in the Lhasa Terrane, Tibet, with implications for understanding the early tectonic history of the Tibetan Plateau. Journal of Sedimentary Research 77, 809–825.

Li, J.X., Qin, K.Z., Li, G.M., Richards, J.P., Zhao, J.X., Cao, M.J., 2014a. Geochronology, geochemistry, and zircon Hf isotopic compositions of Mesozoic

intermediate–felsic intrusions in central Tibet: Petrogenetic and tectonic implications. Lithos 198–199, 77–91.

Li, Y.L., He, J., Wang, C.S., Santosh, M., Dai, J.G., Zhang, Y.X., Wei, Y.S., Wang, J.G., 2013a. Late Cretaceous K-rich magmatism in central Tibet: Evidence for early elevation of the Tibetan plateau? Lithos 160–161, 1–13.

Li, J.X., Qin, K.Z., Li, G.M., Xiao, B., Zhao, J.X., Cao, M.J., Chen, L., 2013b. Petrogenesis of ore-bearing porphyries from the Duolong porphyry Cu–Au deposit, central Tibet: Evidence from U–Pb geochronology, petrochemistry and Sr–Nd–Hf–O isotope characteristics. Lithos 160–161, 216–227.

Li, J.X., Qin, K.Z., Li, G.M., Xiao, B., Zhao, J.X., Chen, L., 2015a. Petrogenesis of Cretaceous igneous rocks from the Duolong porphyry Cu–Au deposit, central Tibet: Evidence from zircon U–Pb geochronology, petrochemistry and Sr–Nd–Pb–Hf isotope characteristics. Geological Journal, doi: 10.1002/gj.2631.

Li, S.M., Zhu, D.C., Wang, Q., Zhao, Z.D., Liu, S.A., 2015b. Southward subduction of the Bangong–Nujiang Tethys: Evidence from the Early Cretaceous volcanic rocks in the northern Lhasa Terrane, central Tibet. To be submitted.

Li, S.M., Zhu, D.C., Wang, Q., Zhao, Z.D., Sui, Q.L., Liu, S.A., Liu, D., Mo, X.X., 2014b. Northward subduction of Bangong-Nujiang Tethys: Insight from Late Jurassic intrusive rocks from Bangong Tso in western Tibet. Lithos 205, 284–297.

Li, X.B., Wang, B.D., Liu, H., Chen, L., Wang, L.Q., 2015d. Petrogenesis of the Middle Jurassic volcanic rocks in Daru Co area, Tibet: Constraints for the subduction of the Bangong-Nujiang oceanic lithosphere. Geological Bulletin of China 34, 251–261 (in Chinese with English abstract).

Li, Y.L., He, J., Meng, J., Wang, C.S., 2015c. Geochronology, petrogenesis and tectonic implications of the Late Jurassic granites from southern Qiangtang terrane, central Tibet. Submitted to Lithos.

Lippert, P.C., van Hinsbergen, D.J.J., Dupont-Nivet, G., 2014. Early Cretaceous to present latitude of the central proto-Tibetan Plateau: A paleomagnetic synthesis with implications for Cenozoic tectonics, paleogeography, and climate of Asia. Geological Society of America Special Paper 507, 1–21.

Liu, D.L., Huang, Q.S., Fan, S.Q., Zhang, L.Y., Shi, R.D., Ding, L., 2014. Subduction of the Bangong–Nujiang Ocean: constraints from granites in the Bangong Co area, Tibet. Geological Journal 49, 188–206.

Liu, S., Hu, R.Z., Gao, S., Feng, C.X., Coulson, I.M., Feng, G.Y., Qi, Y.Q., Yang, Y.H., Yang, C.G., Tang, L., 2012. U–Pb zircon age, geochemical and Sr–Nd isotopic data as constraints on the petrogenesis and emplacement time of andesites from Gerze, southern Qiangtang Block, northern Tibet. Journal of Asian Earth Sciences 45, 150–161.

Liu, W.L., Xia, B., Zhong, Y., Cai, J.X., Li, J.F., Liu, H.F., Cai, Z.R., Sun, Z.L., 2014. Age and composition of the Rebang Co and Julu ophiolites, central Tibet:

Implications for the evolution of the Bangong Meso-Tethys. International Geology Review 56, 430–447.

Loucks, R.R., 1990. Discrimination of ophiolitic from nonophiolitic ultramafic–mafic allochthons in orogenic belts by the Al/Ti ratio in clinopyroxene. Geology 18, 346–349.

Magni, V., van Hunen, J., Funiciello, F., Faccenna, C., 2012. Numerical models of slab migration in continental collision zones. Solid Earth 3, 293–306.

Metcalfe, I., 2013. Gondwana dispersion and Asian accretion: Tectonic and palaeogeographic evolution of eastern Tethys. Journal of Asian Earth Sciences 66, 1–33.

Murphy, M.A., Yin, A., Harrison, T.M., Durr, S.B., Chen, Z., Ryerson, F.J., Kidd, W.S.F., Wang, X., Zhou, X., 1997. Did the Indo-Asian collision alone create the Tibetan plateau? Geology 25, 719–722.

Niu, Y.L., 2014. Geological understanding of plate tectonics: Basic concepts, illustrations, examples and new perspectives. Global Tectonics and Metallogeny 10, 23–46.

Pan, G.T., Ding, J., Yao, D.S., Wang, L.Q., 2004. Guidebook of 1:1,500,000 geological map of the Qinghai–Xizang (Tibet) plateau and adjacent areas. Cartographic Publishing House, Chengdu, China, p. 1–148.

Pan, G.T., Wang, L.Q., Li, R.S., Yuan, S.H., Ji, W.H., Yin, F.G., Zhang, W.P., Wang, B.D., 2012. Tectonic evolution of the Qinghai–Tibet Plateau. Journal of Asian Earth Sciences 53, 3–14.

Pan, G.T., Zheng, H.X., Xu, Y.R., Wang, P.S., Jiao, S.P., 1983. A preliminary study on Bangong Co-Nujiang Suture. Geological memoirs of Qinghai–Xizang Plateau (12)—Geological Tectonics of "Sanjiang". Geological Publishing House, Beijing, p. 229–242 (in Chinese with English abstract).

Pearce, J.A., Mei, H.J., 1988. Volcanic rocks of the 1985 Tibet Geotraverse: Lhasa to Golmud. Philosophical Transactions of the Royal Society of London, Series A, Mathematical and Physical Sciences 327, 169–201.

Pearce, J.A., Norry, M.J., 1979. Petrogenetic implications of Ti, Zr, Y and Nb variations in volcanic rocks. Contributions to Mineralogy and Petrology 69, 33–47.

Ran, H., Wang, G.H., Liang, X., Zheng, Y.L., Jiumi, D., 2015. The Late Jurassic diorite in Rongma area, southern Qiangtang terrane, Tibetan Plateau: Product of northward subduction of the Bangong Co-Nujiang River Tethys Ocean. Geological Bulletin of China 34, 815–825 (in Chinese with English abstract).

Raterman, N.S., Robinson, A.C., Cowgill, E.S., 2014. Structure and detrital zircon geochronology of the Domar fold-thrust belt: Evidence of pre-Cenozoic crustal thickening of the western Tibetan Plateau. Geological Society of America Special Paper 507, 89–114.

Rusmore, M.E., Woodsworth, G.J., Gehrels, G.E., 2005. Two-stage exhumation of midcrustal arc rocks, Coast Mountains, British Columbia. Tectonics, 24, TC5013, doi: 10.1029/2004TC001750.

Schellart, W.P., Lister, G.S., Toy, V.G., 2006. A Late Cretaceous and Cenozoic reconstruction of the Southwest Pacific region: Tectonics controlled by subduction and slab rollback processes. Earth-Science Reviews, 76, 191–233.

Sengör, A.M.C., 1987. Tectonics of the Tethysides: Orogenic collage development in a collisional setting. Annual Review of Earth and Planetary Sciences 15, 213–244.

Soesoo, A., Bons, P.D., Gray, D.R., Foster, D.A., 1997. Divergent double subduction: tectonic and petrologic consequences. Geology 25, 755–758.

Sui, Q.L., Wang, Q., Zhu, D.C., Zhao, Z.D., Chen, Y., Santosh, M., Hu, Z.C., Yuan, H.L., Mo, X.X., 2013. Compositional diversity of ca. 110 Ma magmatism in the northern Lhasa Terrane, Tibet: Implications for the magmatic origin and crustal growth in a continent-continent collision zone. Lithos 168–169, 144–159.

Sun, L.X., 2005. Late Jurassic–Cretaceous sedimentary response to collision process in middle Bangonghu-Nujiang suture. A Dissertation Submitted to China University of Geosciences for Doctoral Degree, Beijing, p. 1–121 (in Chinese with English abstract).

Sun, Y.K., 2010. On the metamorphism and its tectonic significance in Gangdise orogenic zone of Qinghai-Tibet Plateau. A dissertation submitted to Chengdu University of Technology for Master Degree, p. 27–36.

van de Zedde, D.M.A., Wortel, M.J.R., 2001. Shallow slab detachment as a transient source of heat at midlithospheric depth. Tectonics 20, 868–882.

Volkmer, J.E., Kapp, P., Horton, B.K., Gehrels, G.E., Minervini, J.M., Ding, L., 2014. Northern Lhasa thrust belt of central Tibet: Evidence of Cretaceous–early Cenozoic shortening within a passive roof thrust system? Geological Society of America Special Paper 507, 59–70.

Wang, L.Q., Pan, G.T., Ding, J., Yao, D.S., 2013. Guidebook of 1:1,500,000 geological map of the Qinghai–Xizang (Tibet) plateau and adjacent areas. Beijing, China, Geological Publishing House, p. 1–288.

Wang, M.Z., Dong, D.Y., 1984. Stromatoporoids from the Dongqiao Formation (Upper Jurassic–Lower Cretaceous) in northern Xizang (Tibet). Acta Palaeontologica Sinica 23,343–352 (in Chinese with English abstract).

Wang, W.L., Aitchison, J.C., Lo, C.H., Zeng, Q.G., 2008. Geochemistry and geochronology of the amphibolite blocks in ophiolitic mélanges along Bangong–Nujiang suture, central Tibet. Journal of Asian Earth Sciences 33, 122–138.

Wang, Y.S., Zhang, S.Q., Xie, Y.H., Li, C.Z., Yu, X.W., Zheng, C.Z., 2006. 1:250, 000 geological report of Padu Tso with geological map. Jilin Institute of Geological Survey, Changchun, 13–66 (unpublished, in Chinese).

Wen, S.X., 1979. New materials of strata from north of Tibet. Journal of Stratigraphy 3, 150–156 (in Chinese with English abstract).

Wilson, J.T., 1966. Did the Atlantic close and then re-open? Nature 211, 676–681.

Xia, D.X., Liu, S.K. (compiler), 1997. Lithostratigraphy of Xizang Autonomous Region. Wuhan: China University of Geosciences Press, p. 1–302 (in Chinese).

Xiao, W.J., Windley, B.F., Hao, J., Zhai, M.G., 2003. Accretion leading to collision and the Permian Solonker suture, Inner Mongolia, China: termination of the Central Asian orogenic belt. Tectonics 22, 1–20.

Xu, R.H., Schärer, U., Allègre, C.J., 1985. Magmatism and metamorphism in the Lhasa block (Tibet): A geochronological study. Journal of Geology 93, 41–57.

Yin, A., Harrison, T. M., 2000. Geologic evolution of the Himalayan Tibetan Orogen. Ann. Rev. Earth Planet. Sci. 28, 211–280.

Yin, J., Xu, J., Liu, C., Li, H., 1988, The Tibetan plateau: Regional stratigraphic context and previous work. Royal Society of London Philosophical Transactions 327, 5–52.

Zeng, M., Zhang, X., Cao, H., Ettensohn, F.R., Cheng, W.B., Lang, X.H., 2015. Late Triassic initial subduction of the Bangong-Nujiang Ocean beneath Qiangtang revealed: Stratigraphic and geochronological evidence from Gaize, Tibet. Basin Research, 1–11, doi: 10.1111/bre.12105.

Zhang, K.J., 2004. Secular geochemical variations of the Lower Cretaceous siliciclastic rocks from central Tibet (China) indicate a tectonic transition from

continental collision to back-arc rifting. Earth and Planetary Science Letters 229, 73–89.

Zhang, K.J., Xia. B., Zhang, Y.X., Liu, W.L., Zeng, L., Li, J.F., Xu, L.F., 2014b. Central Tibetan Meso-Tethyan oceanic plateau. Lithos 210–211, 278–288.

Zhang, K.J., Zhang, Y.X., Tang, X.C., Xia, B., 2012a. Late Mesozoic tectonic evolution and growth of the Tibetan plateau prior to the Indo-Asian collision. Earth-Science Reviews 114, 236–249.

Zhang, K.J., Zhang, Y.X., Tang, X.C., Xie, Y.W., Sha, S.L., Peng, X.J., 2008. First report of eclogites from central Tibet, China: Evidence for ultradeep continental subduction prior to the Cenozoic India-Asian collision. Terra Nova 20, 302–308.

Zhang, X.R., Shi, R.D., Huang, Q.S., Liu, D.L., Cidan, S.L., Yang, J.S., Ding, L., 2010. Finding of high-pressure mafic granulites in the Amdo terrane, central Tibet. Chinese Science Bulletin 55, 3694–3702.

Zhang, X.R., Shi, R.D., Huang, Q.S., Liu, D.L., Gong, X.H., Chen, S.S., Wu, K., Yi, G.D., Sun, Y.L., Ding, L., 2014a. Early Jurassic high-pressure metamorphism of the Amdo terrane, Tibet: Constraints from zircon U–Pb geochronology of mafic granulites. Gondwana Research 26, 975–985.

Zhang, Z.M., Dong, X., Liu, F., Lin, Y.H., Yan, R., Santosh, M., 2012b. Tectonic evolution of the Amdo terrane, central Tibet: Petrochemistry and zircon U–Pb geochronology. Journal of Geology 120, 431–451.

Zhao, G.C., 2015. Jiangnan Orogen in South China: Developing from divergent double subduction. Gondwana Research 27, 1173–1180.

Zheng, Y.Y., He, J.S., Li, W.J., Zou, G.Q., Zhao, P.J., Ciqiong, Zerenzaxi, Xu, R.K., 2003. 1:250, 000 geological report of Zige Tang Tso with geological map. Xizang Institute of Geological Survey, Lhasa, 90–98 (unpublished, in Chinese).

Zhu, D.C., Pan, G.T., Mo, X.X., Wang, L.Q., Liao, Z.L., Zhao, Z.D., Dong, G.C., Zhou, C.Y., 2006a. Late Jurassic–Early Cretaceous geodynamic setting in middle–northern Gangdese: New insights from volcanic rocks. Acta Petrologica Sinica 22, 534–546 (in Chinese with English abstract).

Zhu, D.C., Pan, G.T., Mo, X.X., Wang, L.Q., Zhao, Z.D., Liao, Z.L., Geng, Q.R., Dong, G.C., 2006b. Identification for the Mesozoic OIB-type basalts in central Qinghai-Tibetan Plateau: Geochronology, Geochemistry and their tectonic setting. Acta Geol Sinica 80, 1312–1328 (in Chinese with English abstract).

Zhu, D.C., Mo, X.X., Niu, Y.L., Zhao, Z.D., Wang, L.Q., Liu, Y.S., Wu, F.Y., 2009. Geochemical investigation of Early Cretaceous igneous rocks along an east–west traverse throughout the central Lhasa Terrane, Tibet. Chemical Geology 268, 298–312.

Zhu, D.C., Zhao, Z.D., Niu, Y.L., Dilek, Y., Hou, Z.Q., Mo, X.X., 2013. The origin and pre-Cenozoic evolution of the Tibetan Plateau. Gondwana Research 23, 1429–1454.

Zhu, D.C., Zhao, Z.D., Niu, Y.L., Mo, X.X., Chung, S.L., Hou, Z.Q., Wang, L.Q., Wu, F.Y., 2011. The Lhasa Terrane: Record of a microcontinent and its histories of drift and growth. Earth and Planetary Science Letters 301, 241–255.

Figure captions

Fig. 1 (a) Tectonic outline of the Tibetan Plateau (Zhu et al., 2013) showing the location of the Bangong suture zone (red dashed line). (b) Simplified geological map showing the distinct Jurassic–Cretaceous geological records within Lhasa-Qiangtang collision zone (Adapted from Wang et al., 2013). Age data sources: Western Qiangtang (Li et al., 2013b, 2014a, 2014b, 2014c, 2015a; Ran et al., 2015); Bangong suture zone (Zhu et al., 2006; Fan et al., 2014); Northern Lhasa (Kapp et al., 2007; Zhu et al., 2011; Chen et al., 2014; Li et al., 2015b; this study). (c–f) Photos showing field occurrences of magmatic rocks in the northern Lhasa subterrane.

Fig. 2 Generalized tectonostratigraphic columns for the Lhasa-Qiangtang collision zone showing the lithostratigraphical units and their relations (Adapted from Zheng et al., 2003; Chen et al., 2005; Wang et al., 2006, 2013; Raterman et al., 2014). See text for details.

Fig. 3 (a) Plots of $\varepsilon_{Hf}(t)$ vs. U-Pb ages of the granitoids from the western Qiangtang subterrane (cf. Li et al., 2013b, 2014a, 2015a; Fan et al., 2015). (b) Th vs. Co plot (Hastie et al., 2007) for the volcanic rocks from the western Qiangtang and northern Lhasa subterranes. Data of Duobuza (Li et al., 2014; Fu et al., 2015), Rena Tso (Liu et al., 2012), and Yanhu (Sui et al., 2013; Zhu et al., 2011). (c) Plots of $\varepsilon_{Hf}(t)$ vs. U-Pb ages of the granitoids from the

Baingoin Batholith in the northern Lhasa subterrane (Table S2, this study). (d) Al_Z (percentage of tetrahedral sites occupied by Al) vs. TiO_2 of clinopyroxene from the Yanhu volcanic rocks in the northern Lhasa subterrane (Table S3, this study). Trends in arc- and rift-related are from Loucks (1990).

Fig. 4 Plot of Zr/Y vs. δNb of the 120–110 Ma basalts from the Bangong suture zone. δNb was calculated following the method of Fitton et al. (1997) [= log (Nb/Y) + 1.74 − 1.92 × log (Zr/Y)]. Data sources: Duoma and Tarenben (Zhu et al., 2006); Zhonggang (Fan et al., 2014); Julu (Liu et al., 2014); Seamounts near the East Pacific Rise (Niu and Batiza, 1997).

Fig. 5 Schematic illustrations showing the closure of the Bangong Ocean driven by a divergent double-sided subduction system in the central Tibet during the Jurassic–Early Cretaceous (not to scale). Paleolatitude data of the southern margin of the Qiangtang Terrane are from Chen et al. (2015) and of the northern margin of the Lhasa Terrane are inferred from Lippert et al. (2014). See text for details.

Zhu et al. Figure 1: W235 mm - H122 mm

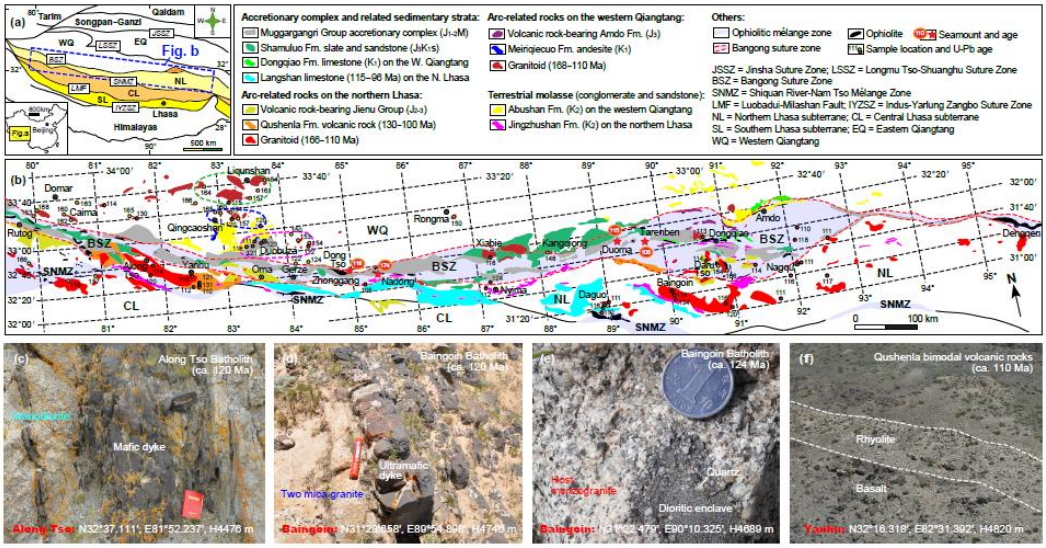

Zhu et al. Figure 2: W170 mm - H105 mm

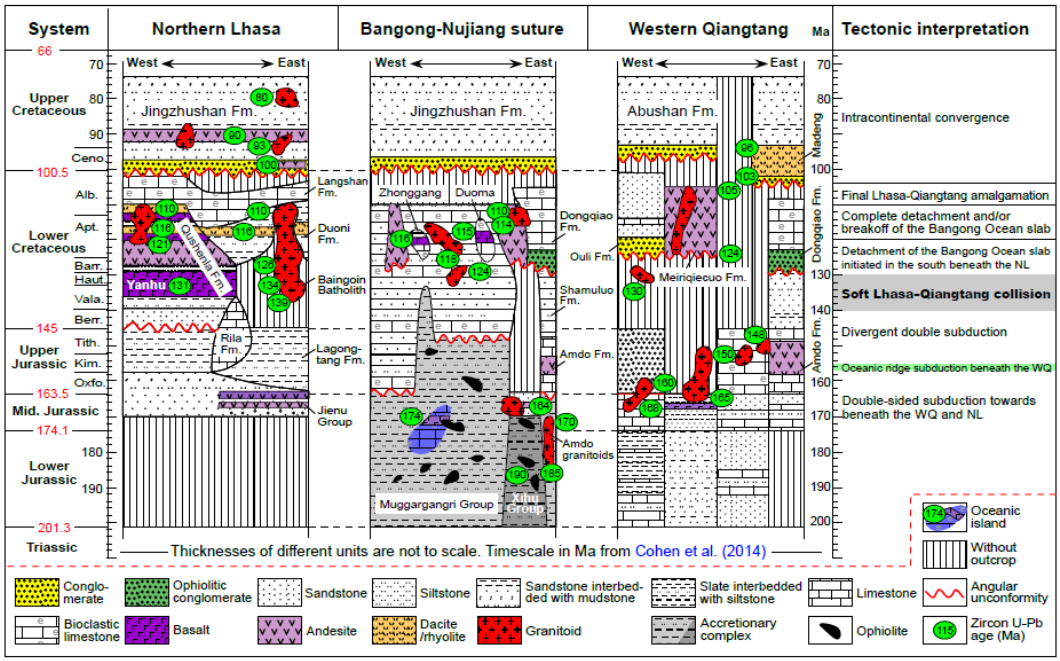

Zhu et al. Figure 3: W160 mm - H120 mm

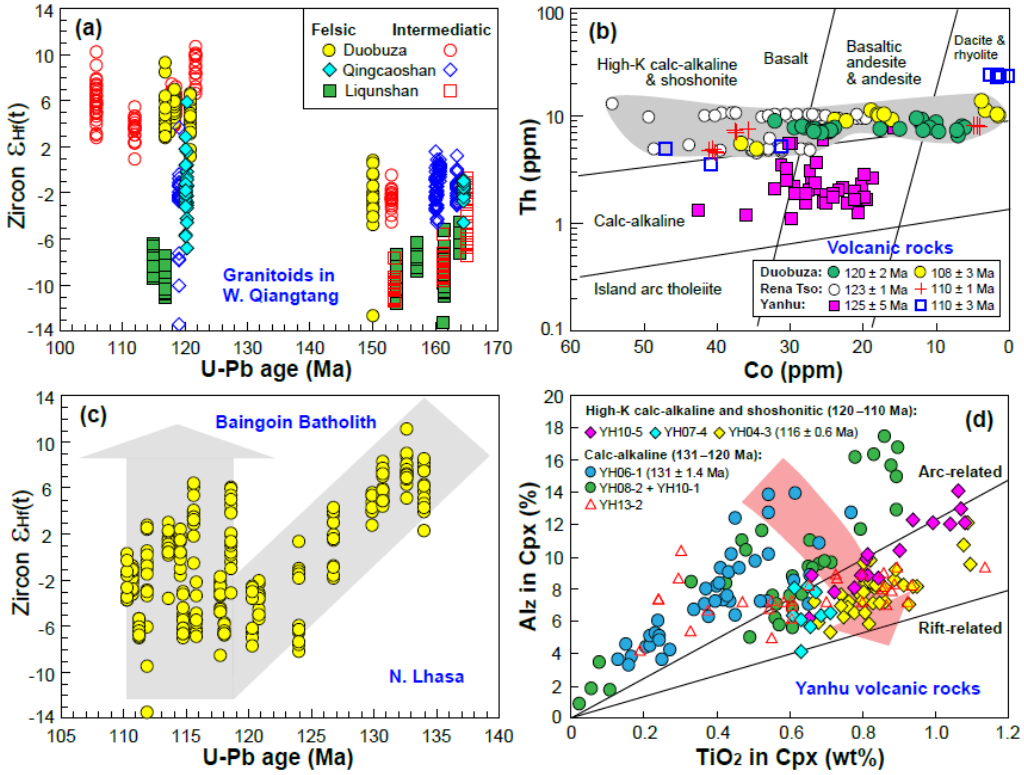

Zhu et al. Figure 4: W80 mm - H60 mm

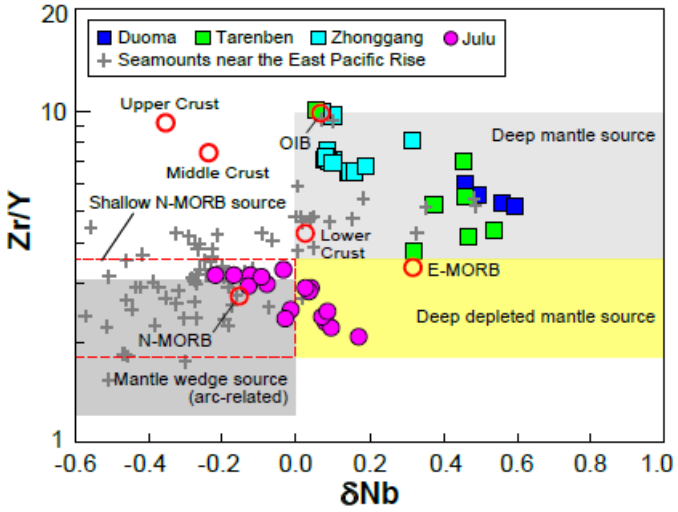

Zhu et al. Figure 5: W160 mm - H110 mm

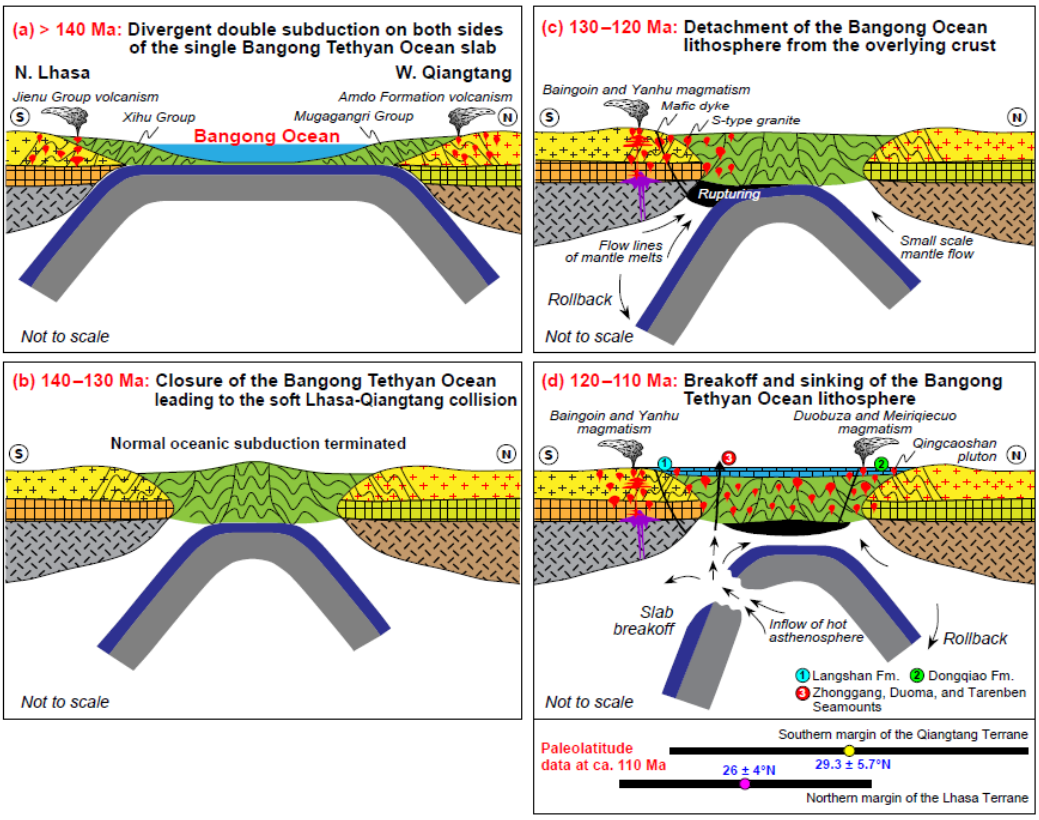

Research Highlights

- ►Two magmatic arcs on the opposing overriding Lhasa and Qiangtang terranes
- ►Extensive 120–110 Ma magmatism with enhanced mantle contributions
- ►Absence of Early Cretaceous high-grade metamorphic rocks
- ►Divergent double-sided subduction of the Bangong oceanic lithosphere